

# Microscopic derivation of the drift velocity and diffusion coefficients in discrete drift-diffusion models of weakly coupled superlattices

L. L. Bonilla

*Departamento de Matemáticas, Escuela Politécnica Superior, Universidad Carlos III de Madrid,  
Avenida de la Universidad 30, 28911 Leganés, Spain  
Also: Unidad Asociada al Instituto de Ciencia de Materiales (CSIC)*

G. Platero and D. Sánchez

*Instituto de Ciencia de Materiales (CSIC), Cantoblanco, 28049 Madrid, Spain  
(January 26, 2019)*

A discrete drift-diffusion model is derived from a microscopic sequential tunneling model of charge transport in weakly coupled SL provided temperatures are low enough. For large biases the diffusion coefficient vanishes and a well known discrete drift model is recovered. Boundary conditions are also derived from microscopic expressions. These conditions clarify when possible self-sustained oscillations of the current are due to monopole or dipole recycling.

72.20.Ht, 73.50.Fq, 73.40.-c

## I. INTRODUCTION

At present, the theory of charge transport and pattern formation in superlattices (SL) is in a fragmentary state. On the one hand, it is possible to establish a quantum kinetic theory from first principles by using Green function formalisms [1,2]. However, the resulting equations are hard to solve, even numerically, unless a number of simplifications and assumptions are made [2,3]. These include: (i) a constant electric field, (ii) simplified scattering models, and (iii) a stationary current through the SL. These assumptions directly exclude the description of electric field domains and their dynamics although important results are still obtained [3,4]. The stationary current density probes the difference between strongly and weakly coupled SL. It also indicates when simpler theories yield good agreement with quantum kinetics. The main simpler theories are (see Figure 1 of Ref. [3]): (i) Semiclassical calculations of miniband transport using the Boltzmann transport equation [5] or simplifications thereof, such as hydrodynamic [6] or drift-diffusion [7] models. These calculations hold for strongly coupled SL at low fields. In the miniband transport regime, electrons traverse the whole SL miniband thereby performing Bloch oscillations and giving rise to negative differential conductivity (NDC) for large enough electric fields [8]. The latter may cause self-sustained oscillations of the current due to recycling of charge dipole domains as in the Gunn effect of bulk n-GaAs [9,6]. (ii) Wannier-Stark (WS) hopping transport in which electrons move parallel to the electric field through scattering processes including hopping transitions between WS levels [10]. Calculations in this regime hold for intermediate fields, larger than those corresponding to collisional broadening of WS levels, but lower than those corresponding to resonant tunneling. (iii) Sequential tunneling calculations valid for weakly

coupled SL (coherence length smaller than one SL period) at basically any value of the electric field [11–13].

On the other hand, the description of electric field domains and self-sustained oscillations in SL has been made by means of discrete drift models. These models use simplified forms of the tunneling current through SL barriers and discrete forms of the charge continuity and Poisson equations [14–16]. Although discrete drift models yield good descriptions of nonlinear phenomena in SL, bridging the gap between them and more microscopic descriptions [12,13] is greatly desirable for further advancing both theory and experiments.

A step in this direction is attempted in the present paper. We consider a weakly coupled SL described by discrete Poisson and charge continuity equations. In the latter the tunneling current through a barrier is a function of the electrochemical potentials of adjacent wells and the potential drops in them and in the barrier. This function is derived by means of the Transfer Hamiltonian method provided the intersubband scattering and the tunneling time are much smaller than the typical dielectric relaxation time [12]. From this microscopic model, we derive a discrete drift-diffusion model and appropriate boundary conditions in the limit of low temperatures. For fields higher than that of the first resonance, the diffusion coefficient is zero, and we obtain the discrete drift model used in previous papers [15–17]. There is one important difference though: drift velocity and boundary condition at the emitter region are now derived microscopically. Thus we arrive at discrete drift-diffusion equations whose velocity and diffusion coefficients are nonlinear functions of the electric field which can be calculated from first principles for any weakly coupled SL. These equations are simpler to study than those of microscopic models and may be useful to understand more deeply the results of numerical simulation thereof [18]. For fields larger than that of the first resonance, the diffusion vanishes and we

obtain the discrete drift model which already describes well many interesting phenomena in weakly coupled SL [15–17].

The rest of the paper is as follows. In Section II, we review the microscopic sequential resonant tunneling model. We obtain the minimal set of independent equations and boundary conditions describing this model. Our derivation of the discrete drift-diffusion model is presented in Section III. Numerical evaluation of velocity, diffusion and contact coefficients for several SLs is presented in Section IV. Section V contains our conclusions.

## II. MICROSCOPIC SEQUENTIAL TUNNELING MODEL

The main charge transport mechanism in a weakly coupled SL is sequential resonant tunneling. We shall assume that the macroscopic time scale of the self-sustained oscillations is larger than the tunneling time (defined as the time an electron needs to advance from one well to the next one). In turn, this latter time is supposed to be much larger than the intersubband scattering time. This means that we can assume the process of tunneling across a barrier to be stationary, with well-defined Fermi-Dirac distributions at each well, which depend on the instantaneous values of the electron density and potential drops. These densities and potentials vary only on the longer macroscopic time scale.

### A. Tunneling current

The tunneling current density across each barrier in the SL may be approximately calculated by means of the Transfer Hamiltonian method. We shall only quote the results here [12]. Let  $eJ_{e,1}$  and  $eJ_{N,c}$  be the currents in the emitter and collector contacts respectively, and let  $eJ_{i,i+1}$  be the current through the  $i$ th barrier which separates wells  $i$  and  $i+1$ . We have

$$J_{e,1} \equiv J_{0,1} = \frac{k_B T}{2\pi^2 \hbar} \sum_{j=1}^n \int A_{Cj}^1(\epsilon) B_{0,1}(\epsilon) T_0(\epsilon) \times \ln \left[ \frac{1 + e^{\frac{\epsilon - \epsilon_{\omega_1} - \epsilon}{k_B T}}}{1 + e^{\frac{\epsilon - \epsilon_{\omega_1+1} - \epsilon}{k_B T}}} \right] d\epsilon, \quad (1)$$

$$J_{i,i+1} = \frac{\hbar k_B T}{2\pi^2 m^*} \sum_{j=1}^n \int A_{C1}^i(\epsilon) A_{Cj}^{i+1}(\epsilon) B_{i-1,i}(\epsilon) \times B_{i,i+1}(\epsilon) T_i(\epsilon) \ln \left[ \frac{1 + e^{\frac{\epsilon - \epsilon_{\omega_i} - \epsilon}{k_B T}}}{1 + e^{\frac{\epsilon - \epsilon_{\omega_{i+1}} - \epsilon}{k_B T}}} \right] d\epsilon, \quad (2)$$

$$J_{N,c} \equiv J_{N,N+1} = \frac{k_B T}{2\pi^2 \hbar} \int A_{C1}^N(\epsilon) B_{N-1,N}(\epsilon)$$

$$\times T_N(\epsilon) \ln \left[ \frac{1 + e^{\frac{\epsilon - \epsilon_{\omega_N} - \epsilon}{k_B T}}}{1 + e^{\frac{\epsilon - \epsilon_F - \epsilon}{k_B T}}} \right] d\epsilon. \quad (3)$$

In these expressions:

- $i = 1, \dots, N-1$ ,  $n$  is the number of subbands in each well  $i$  with energies  $\epsilon_{Cj}^i$  (measured with respect to the common origin of potential drops:  $\epsilon = 0$  at the bottom of the emitter conduction band).  $\epsilon_F = \hbar^2 (3\pi^2 N_D)^{2/3} / (2m^*)$  are the Fermi energies of the emitter and collector regions calculated as functions of their doping density  $N_D$ . Notice that the barrier separating the emitter from the SL is labelled by the index 0, not 1 as in Ref. [12].

- $B_{i-1,i}$  are given by

$$B_{i-1,i} = \frac{k_i}{w + \alpha_{i-1}^{-1} + \alpha_i^{-1}}, \quad (4)$$

$$\hbar k_i = \sqrt{2m^* e \left[ \frac{\epsilon}{e} + W_i \right]}, \quad (5)$$

$$\hbar \alpha_i = \sqrt{2m^* e \left[ V_b - W_i - V_i - \frac{\epsilon}{e} \right]}, \quad (6)$$

$$W_i \equiv V_0 + \sum_{j=1}^{i-1} (V_j + V_{wj}) + V_{wi}, \quad (7)$$

where  $k_i$  and  $\alpha_i$  are the wave vectors in the wells and the barriers, respectively; they depend on the electric potential at the  $i$ th well,  $W_i$ .  $V_i$  and  $V_{wi}$ ,  $i = 1, \dots, N$ , are the potential drops at the  $i$ th barrier and well, respectively. The potential drops  $V_0$  and  $V_N$  correspond to the barriers separating the SL from the emitter and collector contacts, respectively.  $eV_b$  is the barrier height in the absence of potential drops.

- $T_i$  given by

$$T_i(\epsilon) = \frac{16 k_i k_{i+1} \alpha_i^2 e^{-2\alpha_i d}}{(k_i^2 + \alpha_i^2)(k_{i+1}^2 + \alpha_i^2)} \quad (8)$$

is the dimensionless transmission probability through the  $i$ th barrier separating wells  $i$  and  $i+1$ .

- $w$  and  $d$  are the widths of wells and barriers respectively.
- The spectral functions of the wells are Lorentzians whose widths correspond to the LO phonon lifetimes ( $\simeq 1\text{-}10$  meV):

$$A_{Cj}^i(\epsilon) = \frac{\gamma}{(\epsilon - \epsilon_{Cj}^i)^2 + \gamma^2} \quad (9)$$

for the  $i$ th well.

- The integration variable  $\epsilon$  takes on values from the bottom of the  $i$ th well to infinity.

Of course this model can be improved by calculating microscopically the self-energies, which could include other scattering mechanisms (e.g. interface roughness, impurity effects [13]) or even exchange-correlation effects (which affect the electron charge distribution in a self-consistent way). We have assumed that the electrons in each well are in local equilibrium with Fermi energies  $\epsilon_{\omega_i}$  which define the electron number densities  $n_i$ :

$$n_i(\epsilon_{\omega_i}) = \frac{m^* k_B T}{\pi \hbar^2} \int A_{C1}^i(\epsilon) \ln \left[ 1 + e^{\frac{\epsilon_{\omega_i} - \epsilon}{k_B T}} \right] d\epsilon. \quad (10)$$

Notice that the complicated dependence of the wave vectors  $k_i$  and  $\alpha_i$  with the potential,  $W_i$ , may be transferred to the Fermi energies by changing variables in the integrals of the system (2) so that the lower limit of integration (the bottom of the  $i$ th well) is zero:  $\epsilon' = \epsilon + e W_i$ . Then the resulting expressions have the same forms as Equations (2) and (10) if  $\epsilon_{Cj}^i$  and  $\epsilon_{\omega_i}$  in them are replaced by

$$\epsilon_{Cj} = \epsilon_{Cj}^i + e W_i, \quad (11)$$

$$\mu_i \equiv \epsilon_{\omega_i} + e W_i, \quad (12)$$

respectively.  $W_i$  is given by (7). The integrations now go from  $\epsilon' = 0$  to infinity. Notice that  $\epsilon_{Cj}$  is independent of the well index  $i$ . Eq. (10) becomes

$$n_i(\mu_i) = \frac{m^* k_B T}{\pi \hbar^2} \int_0^\infty A_{C1}(\epsilon) \ln \left[ 1 + e^{\frac{\mu_i - \epsilon}{k_B T}} \right] d\epsilon. \quad (13)$$

Here  $A_{C1}(\epsilon)$  is obtained by substituting  $\epsilon_{C1}$  (the energy of the first subband measured from the bottom of a given well, therefore independent of electrostatics) instead of  $\epsilon_{C1}^i$  in (9). Notice that (13) defines a one-to-one relation between  $n_i$  and  $\mu_i$  which is independent of the index  $i$  or the potential drops. The inverse function

$$\mu_i = \mu(n_i, T),$$

gives the chemical potential or free energy per electron. This is the *entropic* part of the electrochemical potential (Fermi energy)

$$\epsilon_{w_i} = \mu(n_i, T) - eV_0 - e \sum_{j=1}^{i-1} (V_j + V_{wj}) - eV_{wi}. \quad (14)$$

According to (14), the Fermi energy,  $\epsilon_{\omega_i}$  (electrochemical potential), is the sum of the electrostatic energy at the  $i$ th well,  $-eW_i = -eV_0 - e \sum_{j=1}^{i-1} (V_j + V_{wj}) - eV_{wi}$ , and the chemical potential,  $\mu_i = \mu(n_i, T)$ .

After the change of variable in the integrals, the wave vectors in (2) become:

$$\begin{aligned} \hbar k_i &= \sqrt{2m^* \epsilon}, \\ \hbar \alpha_i &= \sqrt{2m^* (eV_b - eV_i - \epsilon)}, \\ \hbar k_{i+1} &= \sqrt{2m^* (\epsilon + eV_i + eV_{w_{i+1}})}, \\ \hbar \alpha_{i-1} &= \sqrt{2m^* (eV_b + eV_{w_i} - \epsilon)}, \\ \hbar \alpha_{i+1} &= \sqrt{2m^* (eV_b - eV_i - eV_{i+1} - eV_{w_{i+1}} - \epsilon)}, \end{aligned} \quad (15)$$

where now  $\epsilon = 0$  at the bottom of the  $i$ th well. This shows that the tunneling current density,  $J_{i,i+1}$ , in (2) is a function of: the temperature,  $\mu_i$  and  $\mu_{i+1}$  (therefore of  $n_i$  and  $n_{i+1}$ ), the potential drops  $V_i$ ,  $V_{w_i}$ , and  $V_{w_{i+1}}$ :

$$J_{i,i+1} = \tilde{\Xi}(n_i, n_{i+1}, V_i, V_{w_i}, V_{w_{i+1}}). \quad (16)$$

Similarly, we have

$$J_{e,1} = \tilde{\Xi}_e(n_1, N_D, V_0, V_{w_1}), \quad (17)$$

$$J_{N,c} = \tilde{\Xi}_c(n_N, N_D, V_N, V_{w_N}). \quad (18)$$

## B. Balance and Poisson equations

The 2D electron densities evolve according to the following rate equations:

$$\frac{dn_i}{dt} = J_{i-1,i} - J_{i,i+1} \quad i = 1, \dots, N. \quad (19)$$

The voltage drops through the structure are calculated as follows. The Poisson equation yields the potential drops in the barriers,  $V_i$ , and the wells,  $V_{wi}$  (see Fig. 1):

$$\frac{V_{w_i}}{w} = \frac{V_{i-1}}{d} + \frac{e(n_i - N_D^w)}{2\epsilon}, \quad (20)$$

$$\frac{V_i}{d} = \frac{V_{i-1}}{d} + \frac{e(n_i - N_D^w)}{\epsilon}, \quad (21)$$

where  $\epsilon$  is the GaAs static permittivity,  $n_i$  is the 2D (areal) electron number density (to be determined) which is singularly concentrated on a plane located at the end of the  $i$ th well, and  $N_D^w$  is the 2D intentional doping at the wells.

## C. Boundary conditions

The emitter and collector layers can be described by the following equations:

$$\frac{\Delta_1}{\delta_1} = \frac{eV_0}{d}, \quad \sigma_e = 2\epsilon \frac{V_0}{d} \simeq eN(\epsilon_F)\Delta_1\delta_1, \quad (22)$$

$$\frac{\Delta_2}{e\delta_2} = \frac{V_N}{d} - \frac{1}{2\epsilon} eN_D\delta_2 = \frac{\epsilon_F}{e\delta_3}, \quad (23)$$

$$\sigma_c = 2\epsilon \frac{\epsilon_F}{e\delta_3} = eN_D \left( \delta_2 + \frac{1}{2}\delta_3 \right). \quad (24)$$

To write the emitter equations (22), we assume that there are no charges in the emitter barrier [19]. Then the electric field across  $\delta_1$  (see Fig. 1) is equal to that in the emitter barrier. Furthermore, the areal charge density  $\sigma_e$  required to create this electric field is provided by the emitter.  $N(\epsilon_F) = m^* \hbar^{-2} (3N_D/\pi^4)^{\frac{1}{3}}$  is the density of states

at the emitter Fermi energy  $\epsilon_F = \hbar^2(3\pi^2N_D)^{2/3}/(2m^*)$ . The collector equations (23) and (24) ensure that the electrons tunneling through the  $N$ th (last) barrier are captured by the collector. They hold if the bias is large enough (see below). We assume that: (i) the region of length  $\delta_2$  in the collector is completely depleted of electrons, (ii) there is local charge neutrality in the region of length  $\delta_3$  between the end of the depletion layer  $\delta_2$  and the collector, and (iii) the areal charge density  $\sigma_c$  required to create the local electric field is supplied by the collector. Notice that  $eN_D(\delta_2 + \frac{1}{2}\delta_3)$  in (24) is the positive 2D charge density depleted in the collector region. Equations (23) and (24) hold provided  $V_N \geq \epsilon_F d/(e\delta_3)$ ,  $\Delta_2 \geq 0$ ,  $\delta_2 \geq 0$  and  $\delta_3 \geq 0$ . For smaller biases resulting in  $V_N < \epsilon_F d/(e\delta_3)$ , a boundary condition similar to (22) should be used instead of (23) and (24):

$$\frac{\Delta_2}{\delta_2} = \frac{eV_N}{d}, \quad \sigma_c = 2\varepsilon \frac{V_N}{d} \simeq eN(\epsilon_F)\Delta_2\delta_2. \quad (25)$$

The condition of overall voltage bias closes the set of equations:

$$V = \sum_{i=0}^N V_i + \sum_{i=1}^N V_{wi} + \frac{\Delta_1 + \Delta_2 + \epsilon_F}{e}. \quad (26)$$

This condition holds only if  $V_N \geq \epsilon_F d/(e\delta_3)$ ; otherwise the term  $\epsilon_F/e$  should be omitted in (26).

Notice that we can find  $\delta_1$  and  $\Delta_1$  as functions of  $V_0$  from (22):

$$\Delta_1 = 0 = V_0, \quad \delta_1 \text{ indetermined or} \\ \delta_1 = \sqrt{\frac{2\varepsilon}{e^2 N(\epsilon_F)}} = \frac{\hbar\pi^{2/3}(2\varepsilon)^{1/2}}{em^{*1/2}(3N_D)^{1/6}}, \quad \Delta_1 = \frac{eV_0\delta_1}{d}. \quad (27)$$

Similarly we can find  $\delta_3$  by solving (23) and (24) in terms of  $V_N$  and  $N_D$ . From this equation and (23), we can find  $\delta_2$  and  $\Delta_2$  as functions of  $V_N$ :

$$\delta_3 = \frac{2\varepsilon}{eN_D d} \left[ \sqrt{V_N^2 + \frac{2\epsilon_F N_D d^2}{\varepsilon}} - V_N \right], \\ \delta_2 = \frac{2\varepsilon\epsilon_F}{e^2 N_D \delta_3} \left( \frac{eV_N \delta_3}{\epsilon_F d} - 1 \right) \theta \left( \frac{eV_N \delta_3}{\epsilon_F d} - 1 \right), \\ \Delta_2 = \frac{2\varepsilon\epsilon_F^2}{e^2 N_D \delta_3^2} \left( \frac{eV_N \delta_3}{\epsilon_F d} - 1 \right) \theta \left( \frac{eV_N \delta_3}{\epsilon_F d} - 1 \right), \quad (28)$$

where  $\theta(x)$  is the Heaviside unit step function. Thus the potential drops at the barriers separating the SL from the contact regions uniquely determine the contact electrostatics.

In Ref. [12] global charge conservation:

$$\sigma_e + \sum_{i=1}^N (n_i - eN_D^w) = eN_D(\delta_2 + \frac{1}{2}\delta_3), \quad (29)$$

was used instead of (24) [which is a condition similar to the one we impose at the emitter contact, (22)]. Substitution of (24) instead of (29) modifies minimally the numerical results reported in Refs. [12] and [18].

#### D. Elimination of the potential drops at the wells

The previous model has too many equations. We can eliminate the potential drops at the wells from the system. For (20) and (21) imply

$$\frac{V_{wi}}{w} = \frac{V_{i-1} + V_i}{2d}. \quad (30)$$

Then the bias condition (26) becomes

$$V = \left(1 + \frac{w}{d}\right) \sum_{i=0}^N V_i - \frac{(V_0 + V_N)w}{2d} + \frac{\Delta_1 + \Delta_2 + \epsilon_F}{e}, \quad (31)$$

where  $\Delta_1 = \Delta_1(V_0)$  and  $\Delta_2 = \Delta_2(V_N)$ . Instead of the rate equations (19), we can derive a form of Ampère's law which explicitly contains the total current density  $J(t)$ . We differentiate (21) with respect to time and eliminate  $n_i$  by using (19). The result is

$$\frac{\varepsilon}{ed} \frac{dV_i}{dt} + J_{i,i+1} = J(t), \quad i = 0, 1, \dots, N, \quad (32)$$

where  $eJ(t)$  is the sum of displacement and tunneling currents. The time-dependent model consists of the  $2N+2$  equations (21), (31) and (32) [the currents are given by Eqs. (2), (10), (27), (28) and (30)], which contain the  $2N+2$  unknowns  $n_i$  ( $j = 1, \dots, N$ ),  $V_j$  ( $j = 0, 1, \dots, N$ ), and  $J$ . Thus we have a system of equations which, together with appropriate initial conditions, determine completely and self-consistently our problem. For convenience, let us list again the minimal set of equations we need to solve in order to determine completely all the unknowns:

$$\frac{\varepsilon}{ed} \frac{dV_i}{dt} + J_{i,i+1} = J(t), \quad i = 0, 1, \dots, N, \quad (33)$$

$$\frac{V_i}{d} = \frac{V_{i-1}}{d} + \frac{e(n_i - N_D^w)}{\varepsilon}, \quad i = 1, \dots, N, \quad (34)$$

$$V = \left(1 + \frac{w}{d}\right) \sum_{i=0}^N V_i - \frac{(V_0 + V_N)w}{2d} + \frac{\Delta_1(V_0) + \Delta_2(V_N) + \epsilon_F}{e}, \quad (35)$$

$$J_{i,i+1} = \Xi(n_i, n_{i+1}, V_{i-1}, V_i, V_{i+1}), \quad (36)$$

$$J_{e,1} = \Xi_e(n_1, V_0, V_1), \quad (37)$$

$$J_{N,c} = \Xi_c(n_N, V_{N-1}, V_N). \quad (38)$$

Notice that the three last equations are constitutive relations obtained by substituting (30) in the functions  $\tilde{\Xi}$ ,

$\tilde{\Xi}_e$  and  $\tilde{\Xi}_c$  of (16), (17) and (18), respectively. The functions  $\Delta_1(V_0)$  and  $\Delta_2(V_N)$  are given by (27) and (28), respectively. Equations (32) for  $i = 0, N$  may be considered the real boundary conditions for the barriers separating the SL from the contacts. Notice that these boundary conditions are just the balance of current density with special tunneling current constitutive relations  $J_{e,1}$  and  $J_{N,c}$  depending on the electron densities at the extreme wells of the SL and the potential drops at the adjacent barriers.

### III. DERIVATION OF THE DISCRETE DRIFT-DIFFUSION MODEL

It is interesting to consider the relation (10) between the chemical potential and the electron density at a well for different temperature ranges:

$$n_i(\mu_i) = \frac{m^* k_B T}{\pi \hbar^2} \int A_{C1}(\epsilon) \ln \left[ 1 + e^{\frac{\mu_i - \epsilon}{k_B T}} \right] d\epsilon.$$

Assuming that  $\mu_i \gg k_B T$ , we may approximate this expression by

$$n_i(\mu_i) \approx \frac{m^*}{\pi \hbar^2} \int_0^{\mu_i} A_{C1}(\epsilon) (\mu_i - \epsilon) d\epsilon.$$

Thus  $n_i$  approaches a linear function of  $\mu_i$  if  $\mu_i \gg k_B T$ . For the SL used in the experiments we have been referring to,  $\mu_i - \epsilon$  is typically about 20 meV or 200 K. Thus “low temperature” can be “high enough temperature” in practice. Provided the Lorentzian  $A_{C1}(\epsilon)$  is sufficiently narrow,  $A_{C1}(\epsilon) \sim \pi \delta(\epsilon - \epsilon_{C1})$ , so that

$$\mu_i - \epsilon_{C1} \approx \frac{\hbar^2 n_i}{m^*} \quad \text{if } \mu_i \gg k_B T, \epsilon_{C1} \gg \gamma. \quad (39)$$

A different approximation is obtained if we first impose that  $\epsilon_{C1} \gg \gamma$ :

$$n_i(\mu_i) \approx \frac{m^* k_B T}{\hbar^2} \ln \left[ 1 + e^{\frac{\mu_i - \epsilon_{C1}}{k_B T}} \right].$$

This yields

$$\mu_i \approx \epsilon_{C1} + k_B T \ln \left[ e^{\frac{\hbar^2 n_i}{m^* k_B T}} - 1 \right],$$

and therefore

$$\begin{aligned} \mu_i - \epsilon_{C1} &\approx \frac{\hbar^2 n_i}{m^*} \quad \text{if } \hbar^2 n_i \gg m^* k_B T, \\ \mu_i - \epsilon_{C1} &\approx k_B T \ln \frac{\hbar^2 n_i}{m^* k_B T} \quad \text{if } \hbar^2 n_i \ll m^* k_B T. \end{aligned}$$

At low temperatures, the chemical potential depends linearly on the electron density, whereas it has ideal gas logarithmic dependence at high temperatures.

The same considerations would indicate that the electron flux across the  $i$ th barrier becomes

$$J_{i,i+1} \approx \frac{n_i v_i^{(f)} - n_{i+1} v_i^{(b)}}{d + w}.$$

Here  $v_i^{(f)}$  and  $v_i^{(b)}$  are functions of  $V_i, V_{i\pm 1}$ . They have dimensions of velocity and correspond to the forward and backward tunneling currents which were invoked in the derivation of phenomenological discrete drift models. When  $\epsilon_{w_i} = \epsilon_{w_{i+1}}$ , or equivalently,  $\mu_{i+1} = \mu_i + eV_i + eV_{w_{i+1}}$ ,  $J_{i,i+1} = 0$  according to (2). Equation (13) implies that  $\mu_{i+1} = \mu_i$  if  $n_{i+1} = n_i$ , and therefore we conclude that  $v_i^{(f)} = v_i^{(b)}$  at zero potential drops  $V_i + V_{w_{i+1}} = 0$ . Notice that  $\epsilon_{w_{i+1}} - \epsilon$  becomes  $\mu_{i+1} - eV_i - eV_{w_{i+1}} - \epsilon'$  after changing variables in the integral (2). Then  $v_i^{(b)}$  is approximately zero unless  $0 < \epsilon_{C1} < \mu_{i+1} - eV_i - eV_{w_{i+1}}$ . For voltages larger than those in the first plateau of the current–voltage characteristic curve this condition does not hold. In fact for these voltages, the level  $C1$  of well  $i$  is at a higher or equal potential than the level  $C2$  of well  $i + 1$ . Then  $\epsilon_{C1} \geq \mu_{i+1} - eV_i - eV_{w_{i+1}}$ .

The previous results yield discrete drift-diffusion models with the potential drops at the barriers and the total current density as unknowns, the same as in Eqs. (33) - (38). The main difference with previously used discrete drift models is that the velocity depends on more than one potential drop. To obtain these simpler models, we further assume that  $V_i/d$  and  $V_{i\pm 1}/d$  are approximately equal to an average field  $F_i$ . This assumption departs from previous approximations and provides us with a new model. The point of contact between this new model and our previous results is that  $e^{-\alpha_i d}$  (appearing in the transmission coefficient) is the controlling factor in the expressions for  $v^{(f)}$  and  $v^{(b)}$ . This controlling factor is uniquely determined by the potential drop at the  $i$ th barrier,  $V_i$ . Thus the behavior of forward and backward drift velocities is most influenced by the potential drop  $V_i \approx F_i d$  and the new drift-diffusion model (see below) should yield results similar to those of the microscopic sequential tunneling model. We have

$$\begin{aligned} J_{i,i+1} &\approx \frac{n_i v^{(f)}(F_i) - n_{i+1} v^{(b)}(F_i)}{d + w} \\ &= \frac{n_i v(F_i)}{d + w} - \frac{n_{i+1} - n_i}{(d + w)^2} D(F_i), \end{aligned} \quad (40)$$

$$v(F) = v^{(f)}(F) - v^{(b)}(F), \quad D(F) = (d + w) v^{(b)}(F). \quad (41)$$

To calculate  $v^{(f)}(F)$  and  $v^{(b)}(F)$  from  $J_{i,i+1}$  in (2), we hold  $V_i = V_{i\pm 1} = F_i d$  after transforming this formula to the form (36). Notice that (as said above)

$$v^{(f)}(0) = v^{(b)}(0) = \frac{D(0)}{d + w}$$

for the tunneling current to vanish at zero field and equal electron densities at adjacent wells. Furthermore, notice

that  $D(F)$  vanishes if  $\epsilon_{C1} \geq \mu_{i+1} - e(d+w)F_i$  since by (30)

$$V_i + V_{w_{i+1}} = [(w+2d)V_i + wV_{i+1}]/(2d) \approx (w+d)F_i.$$

Thus according to (39),  $D(F)$  vanishes if  $\hbar^2 n_{i+1} \leq m^* e(d+w)F_i$ , which is certainly satisfied for all average fields larger than the first resonant field  $(\epsilon_{C2} - \epsilon_{C1})/[e(d+w)]$ . In the low temperature limit, we have

$$\begin{aligned} \Xi(n_i, n_{i+1}, Fd, Fd, Fd) &= \frac{n_i}{d+w} v(F) \\ &- \frac{n_{i+1} - n_i}{(d+w)^2} D(F). \end{aligned} \quad (42)$$

Then we may use

$$v(F) = \frac{(d+w)\Xi(N_D^w, N_D^w, Fd, Fd, Fd)}{N_D^w}, \quad (43)$$

$$D(F) = -\frac{(d+w)^2\Xi(0, N_D^w, Fd, Fd, Fd)}{N_D^w}, \quad (44)$$

to calculate the drift velocity and the diffusion coefficient from the tunneling current.

Equations (42) to (44) may be used in (33) to write the Ampère law as

$$\frac{\varepsilon}{e} \frac{dF_i}{dt} + \frac{n_i v(F_i)}{d+w} - D(F_i) \frac{n_{i+1} - n_i}{(d+w)^2} = J(t), \quad (45)$$

for  $i = 1, \dots, N-1$ . Poisson equation (34) becomes

$$F_i - F_{i-1} = \frac{e}{\varepsilon} (n_i - N_D^w), \quad (46)$$

for  $i = 1, \dots, N$ . Equations (45) and (46) constitute a discrete drift-diffusion model which may be analyzed on its own together with appropriate bias and boundary conditions. As bias condition we adopt

$$(d+w) \sum_{i=1}^{N-1} F_i + (F_0 + F_N) d = V. \quad (47)$$

Notice that we have omitted the potential drops at the contacts for the sake of simplicity. For fields higher than the first resonance,  $D(F) \approx 0$ , and (45) becomes

$$\frac{\varepsilon}{e} \frac{dF_i}{dt} + \frac{n_i v(F_i)}{d+w} = J(t), \quad (48)$$

which is the usual discrete drift model used in previous theoretical studies [15–17].

In Section 2.1 of Ref. [13], A. Wacker derived a formula similar to (40) with  $v^{(b)} = 0$  and  $v^{(f)}(F) \propto \Gamma/[(eF(d+w) + \epsilon_{C1} - \epsilon_{Cj})^2 + \Gamma^2]$ , for fields comparable to  $(\epsilon_{Cj} - \epsilon_{C1})/[e(d+w)]$ . At low fields, the resonant tunneling current between levels  $C1$  of adjacent fields was found to be proportional to  $W(F) = eF(d+w)/[(e^2 F^2 (d+w)^2 + \Gamma^2)]$  and independent of  $n_i$ . While the first approximation of Wacker's (for fields close to higher

resonances,  $C1 \rightarrow Cj$ ,  $j = 2, 3, \dots$ ) is compatible with our result (40), the second approximation is an artifact of the extra unnecessary assumption  $\epsilon_{w_i} = \epsilon_{w_{i+1}}$  [13]. We shall show in Section IV that our drift velocity (43) may have at low fields the same shape as function  $W(F)$  for certain SL; see Fig. 2(a). Then the corresponding stationary current for a space homogeneous field profile with  $n_i = N_D^w$  (which implies equality of chemical potentials at adjacent fields) will be proportional to  $W(F)$  and our result will agree with Wacker's (for this special case). Fig. 2(b) shows that things may be different for a different SL configuration.

The boundary conditions for  $F_0$  and  $F_N$  are also Ampère's law but now the tunneling currents (1) and (3) (from the emitter and to the collector, respectively) have to be used instead of (2). The same approximations as before yield

$$\begin{aligned} J_{e,1} &= \Xi_e(n_1, F_0 d, F_0 d) \\ &\approx j_e^{(f)}(F_0) - \frac{n_1}{d+w} w^{(b)}(F_0), \end{aligned} \quad (49)$$

$$\begin{aligned} J_{N,c} &= \Xi_c(n_N, F_N d, F_N d) \\ &\approx \frac{n_N}{d+w} w^{(f)}(F_N). \end{aligned} \quad (50)$$

Notice that there is no backward tunneling from the collector region to the SL because we are assuming that the potential drop  $V_N$  is larger than  $\epsilon_F d/(e\delta_3)$ . Assuming now that (49) and (50) are identities, we find

$$j_e^{(f)}(F) = \Xi_e(0, Fd, Fd), \quad (51)$$

$$w^{(b)}(F) = \frac{d+w}{N_D^w} [j_e^{(f)}(F) - \Xi_e(N_D^w, Fd, Fd)], \quad (52)$$

$$w^{(f)}(F) = \frac{d+w}{N_D^w} \Xi_c(N_D^w, Fd, Fd). \quad (53)$$

The tunneling current across a barrier is zero if the Fermi energies of the adjacent wells are equal. This occurs if the electron density at the first well takes on an appropriate value  $n_1^w$  such that the corresponding Fermi energy equals that of the emitter. Then

$$\Xi_e(n_1^w, 0, 0) = 0,$$

and therefore

$$j_e^{(f)}(0) = \frac{n_1^w w^{(b)}(0)}{d+w}.$$

#### IV. NUMERICAL CALCULATION OF DRIFT VELOCITY AND DIFFUSION

In this Section, we shall calculate the functions  $v(F)$ ,  $D(F)$ ,  $j_e^{(f)}(F)$ ,  $w^{(b)}(F)$  and  $w^{(f)}(F)$  for different SL used in experiments [17].

Fig. 2(a) depicts the electron drift velocity  $v(F)$  for the 9nm/4nm GaAs/AlAs SL (9/4 SL) of Ref. [17] calculated by means of (43) (at zero temperature). The inset compares  $v(F)$  to the backward and forward velocities given by  $v^{(b)}(F) = D(F)/(d+w)$  [ $D(F)$  as in (44)] and  $v^{(f)}(F) = v(F) + v^{(b)}(F)$ . The rapidly decreasing diffusivity  $D(F)$  determines the position and height of the first peak in  $v(F)$ . Notice that  $v(F)$  is as expected from general considerations: linear for low electric fields, it reaches a maximum and then decays before the influence of the second resonance is felt. If  $D(F)$  decays faster, a rather different  $v(F)$  is found. Fig. 2(b) shows  $v(F)$  for the 13.3/2.7 SL: there is a wide region before the first peak in which  $v''(F) > 0$ .

Figures 3 and 4 show the boundary functions  $j_e^{(f)}(F)$ ,  $w^{(b)}(F)$  and  $w^{(f)}(F)$  for the 9/4 and 13.3/2.7 SL, respectively. They behave as we would have expected: (i) the emitter forward current presents maxima at the resonant values of the electric field [different from those of  $v^{(f)}(F)$ ], (ii) the emitter backward tunnel velocity decreases rapidly with field, and (iii) the collector forward velocity increases monotonically with field given the distance between the Fermi energy of the last well and that of the collector.

The emitter forward current,  $j_e^{(f)}(F)$ , is compared in Figs. 5 and 6 to the drift current,  $N_D^w v(F)/(d+w)$ , for different emitter doping values. Notice that the emitter current is systematically higher than the drift current for large emitter doping. Then the electric field in the SL increases with distance from the emitter and a charge accumulation layer is formed. Self-consistent current oscillations in this situation will be due to monopole recycling [18]. Notice that previous work on discrete drift models assumed a fixed excess of electrons in the first SL well as boundary condition [16,17]. Again an emitter accumulation layer appeared and monopole self-oscillation resulted.

For smaller emitter doping,  $j_e^{(f)}(F)$  intersects  $N_D^w v(F)/(d+w)$  on its second branch, and a charge depletion layer may be formed in the SL. Then there may be self-oscillations due to dipole recycling. These findings are fully consistent with the numerical results reported in Ref. [18] for the 13.3/2.7 SL. That paper reported coexistence and bistability of monopole and dipole self-oscillations for the first time. Coexistence and bistability were found for an intermediate emitter doping range (crossover range) *lower* than those used in experiments [18]. A different way to obtain dipole self-oscillations is to decrease the well width without changing contact doping. In this way, we have numerically checked that dipole self-oscillations are possible with emitter doping similar to those used in current experimental setups [17].

For the usual drift-diffusion model of the Gunn effect in bulk n-GaAs and boundary conditions analogous to the present ones, asymptotic and numerical calculations were performed some time ago [20]. They provide results consistent with our present findings in SL: a boundary con-

dition which yields accumulation (depletion) layer near injecting contact may yield current self-oscillations due to monopole (dipole) recycling [20,21]. However these similarities between discrete (SL) and continuous (bulk) drift-diffusion models should not tempt us into reaching hasty conclusions: discrete and continuous drift-diffusion models may have rather different traveling wave solutions [22]. These differences may have experimentally observable consequences which will be explored elsewhere.

## V. CONCLUSIONS

Starting from a microscopic sequential tunneling model of transport in weakly coupled SL, we have derived a discrete drift-diffusion model in the low temperature limit. For large biases such that the fields in the SL surpass the first resonance, the diffusion coefficient vanishes and we recover a well known discrete drift model [16]. We have also derived boundary conditions for the discrete drift-diffusion model. These conditions clarify when possible self-sustained oscillations of the current are due to monopole or dipole recycling.

## ACKNOWLEDGMENTS

One of us (LLB) thanks Dr. Andreas Wacker for fruitful discussions and collaboration on discrete drift-diffusion models. This work was supported by the Spanish DGES through grants PB97-0088 and PB96-0875, by the European Union TMR contracts ERB FMBX-CT97-0157 and FMRX-CT98-0180 and by the Community of Madrid, project 07N/0026/1998.

---

- [1] L. P. Kadanoff and G. Baym, *Quantum Statistical Mechanics*. (Benjamin, New York, 1962); L. V. Keldysh, Sov. Phys. JETP **20**, 1018 (1965) [Zh. Eksp. Theor. Fiz. **47**, 1515 (1964)].
- [2] H. Haug and A.-P. Jauho, *Quantum Kinetics in Transport and Optics of Semiconductors* (Springer, Berlin 1996).
- [3] A. Wacker and A.-P. Jauho, Phys. Rev. Lett. **80**, 369 (1998).
- [4] A. Wacker, A.-P. Jauho S. Rott, A. Markus, P. Binder and G.H. Döhler, Phys. Rev. Lett. **83**, 836 (1999).
- [5] J. F. Palmier, G. Etemadi, A. Sibille, M. Hadjazi, F. Mollot and R. Planel, Surface Sci. **267**, 574 (1992); R.R. Gerhardts, Phys. Rev. B **48**, 9178 (1993); A.A. Ignatov, E.P. Dodin and V.I. Shashkin, Mod. Phys. Lett. B **5**, 1087 (1991).
- [6] M. Büttiker and H. Thomas, Phys. Rev. Lett. **38**, 78 (1977); Z. Phys. B **34**, 301 (1979); X.L. Lei, N.J.M. Hor-

ing and H.L. Cui, Phys. Rev. Lett. **66**, 3277 (1991); J.C. Cao and X.L. Lei, Phys. Rev. B **60**, 1871 (1999).

[7] A. Sibille, J. F. Palmier, F. Mollot, H. Wang and J. C. Esnault, Phys. Rev. B **39**, 6272 (1989).

[8] L. Esaki and R. Tsu, IBM J. Res. Dev. **14**, 61 (1970).

[9] J. B. Gunn, Solid State Commun. **1**, 88 (1963).

[10] R. Tsu and G.H. Döhler, Phys. Rev. B **12**, 680 (1975); S. Rott, N. Linder and G.H. Döhler, Superlatt. and Microstr. **21**, 569 (1997); S. Rott, P. Binder, N. Linder and G.H. Döhler, Phys. Rev. B **59**, 7334 (1999).

[11] R.F. Kazarinov and R.A. Suris, Fiz. Tekh. Poluprov. **6**, 148 (1972) [Sov. Phys. Semicond. **6**, 120 (1972)].

[12] R. Aguado, G. Platero, M. Moscoso and L.L. Bonilla, Phys. Rev. B **55**, R16053 (1997).

[13] A. Wacker, in *Theory and transport properties of semiconductor nanostructures*, edited by E. Schöll. Chapter 10. Chapman and Hill, New York, 1998.

[14] F. Prengel, A. Wacker and E. Schöll, Phys. Rev. B **50**, 1705 (1994).

[15] L.L. Bonilla, J. Galán, J.A. Cuesta, F.C. Martínez and J. M. Molera, Phys. Rev. B **50**, 8644 (1994).

[16] L.L. Bonilla, in *Nonlinear Dynamics and Pattern Formation in Semiconductors and Devices*, edited by F.-J. Niedernostheide. Pages 1-20. Springer, Berlin, 1995; A. Wacker, M. Moscoso, M. Kindelan and L.L. Bonilla, Phys. Rev. B **55**, 2466 (1997); L.L. Bonilla, M. Kindelan, M. Moscoso, and S. Venakides, SIAM J. Appl. Math. **57**, 1588 (1997).

[17] J. Kastrup, H.T. Grahn, R. Hey, K. Ploog, L.L. Bonilla, M. Kindelan, M. Moscoso, A. Wacker and J. Galán, Phys. Rev. B **55**, 2476 (1997); J.W. Kantelhardt, H. T. Grahn, K. H. Ploog, M. Moscoso, A. Perales and L.L. Bonilla, Physica Status Solidi B **204**, 500 (1997).

[18] D. Sánchez, M. Moscoso, L. L. Bonilla, G. Platero and R. Aguado, Phys. Rev. B **60**, 4489 (1999).

[19] V. J. Goldman, D. C. Tsui and J. E. Cunningham, Phys. Rev. Lett. **58**, 1256 (1987); Phys. Rev. B **35**, 9387 (1987); J. Iñarrea and G. Platero, Europhys. Lett. **33**, 477 (1996).

[20] G. Gomila, J. M. Rubí, I. R. Cantalapiedra and L. L. Bonilla, Phys. Rev. E **56**, 1490 (1997); L. L. Bonilla, I. R. Cantalapiedra, G. Gomila and J. M. Rubí, Phys. Rev. E **56**, 1500 (1997).

[21] M. P. Shaw, H. L. Grubin and P. R. Solomon, *The Gunn-Hilsum effect* (Academic P., New York, 1979).

[22] L. L. Bonilla, E. Schöll and A. Wacker, unpublished.

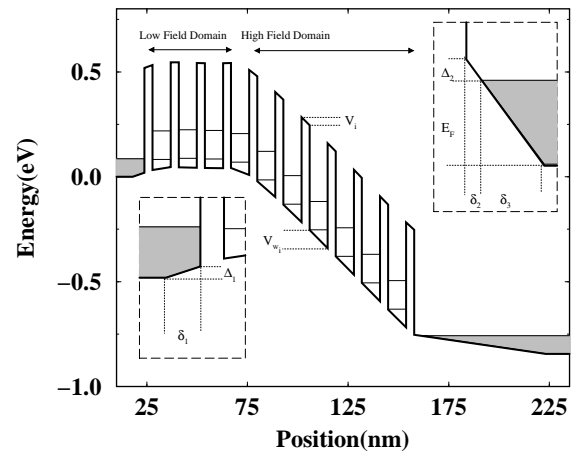


FIG. 1. Sketch of the electrostatic potential profile in a SL.

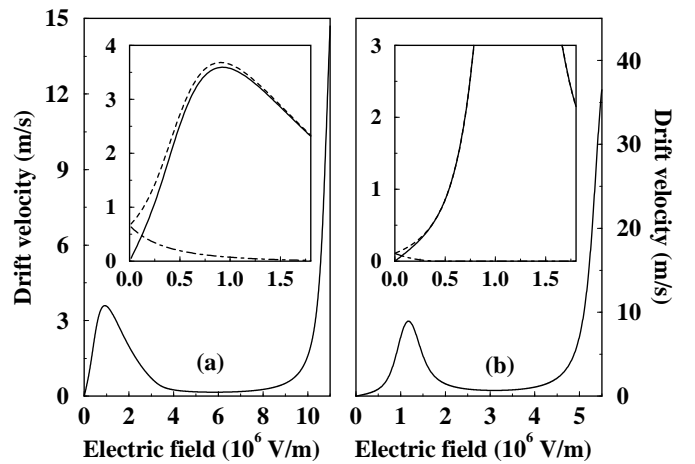


FIG. 2. (a) Electron drift velocity  $v(F)$  for the 9/4 SL. Inset: comparison of the drift velocity (continuous line) with the forward (dashed line) and backward (dot-dashed line) velocities. (b) The same for the 13.3/2.7 SL. Notice that the backward velocity or, equivalently the diffusivity, decreases with electric field much more rapidly for this SL.

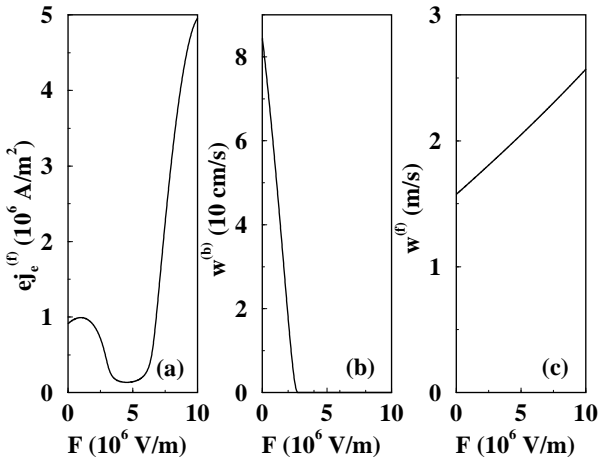


FIG. 3. Functions of the electric field appearing in the boundary conditions for the 9/4 SL with a contact doping  $N_D = 2 \times 10^{18} \text{ cm}^{-3}$ . (a)  $ej_e^{(f)}(F)$  and (b)  $w^{(b)}(F)$  for the emitter and (c)  $w^{(f)}(F)$  for the collector.

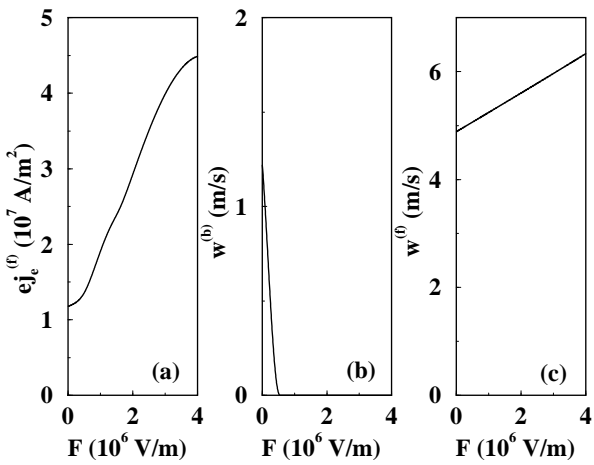


FIG. 4. Same functions as in Figure 3 for the 13.3/2.7 SL with a contact doping  $N_D = 2 \times 10^{18} \text{ cm}^{-3}$ . Notice that  $ej_e^{(f)}(F)$  is an increasing function since  $\epsilon_F > (\epsilon_{C2} - \epsilon_{C1})$  in this SL.

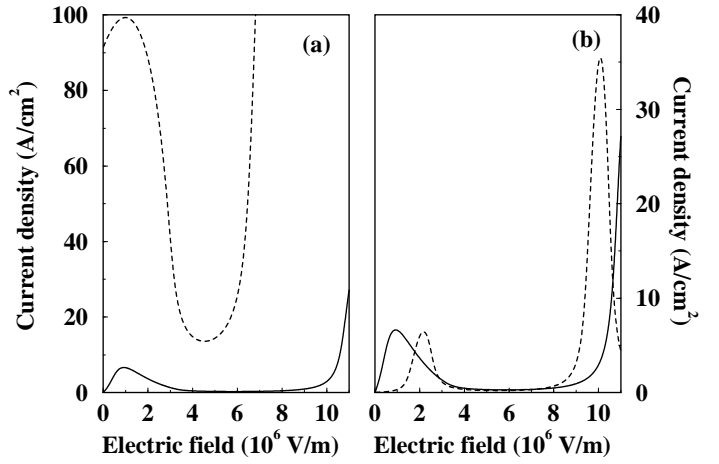


FIG. 5. Comparison of the drift tunneling current density,  $eN_D^w v(F)/(d+w)$  (continuous lines) with the emitter current density  $ej_e^{(f)}(F)$  (dashed lines) for the 9/4 SL with two different emitter dopings: (a)  $N_D = 2 \times 10^{18} \text{ cm}^{-3}$  corresponding to monopole recycling, and (b)  $N_D = 2 \times 10^{17} \text{ cm}^{-3}$  corresponding to dipole recycling.

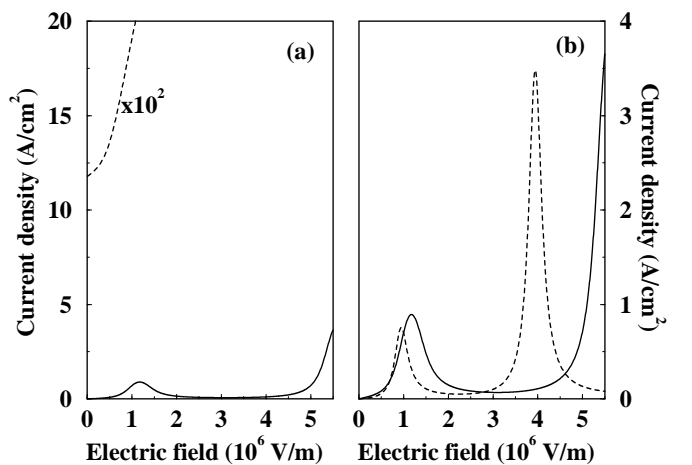


FIG. 6. Same functions as in Figure 5 for the 13.3/2.7 SL (a)  $N_D = 2 \times 10^{18} \text{ cm}^{-3}$  (monopole recycling), and (b)  $N_D = 1 \times 10^{16} \text{ cm}^{-3}$  (dipole recycling).